

See discussions, stats, and author profiles for this publication at: <https://www.researchgate.net/publication/319274438>

Tissue distribution following 28 day repeated oral administration of aluminum-based nanoparticles with different properties and the in vitro toxicity

Article in *Journal of Applied Toxicology* · August 2017

DOI: 10.1002/jat.3509

CITATIONS

7

READS

104

7 authors, including:



Park Eun Jung

Yonsei University

257 PUBLICATIONS 7,608 CITATIONS

[SEE PROFILE](#)



Gwang-Hee Lee

Korea University

81 PUBLICATIONS 1,432 CITATIONS

[SEE PROFILE](#)



Uiseok Jeong

Korea Advanced Institute of Science and Technology

19 PUBLICATIONS 224 CITATIONS

[SEE PROFILE](#)



Jaerak Chang

Ajou University

42 PUBLICATIONS 806 CITATIONS

[SEE PROFILE](#)

Some of the authors of this publication are also working on these related projects:



Electrocatalysts of Li-O₂ batteries [View project](#)



Centrosomal localization and functional characterization of hPlk2 [View project](#)

RESEARCH ARTICLE

Tissue distribution following 28 day repeated oral administration of aluminum-based nanoparticles with different properties and the in vitro toxicity

Eun-Jung Park^{1†}  | Gwang-Hee Lee^{2†} | Cheolho Yoon³ | Uiseok Jeong⁴ |
Younghun Kim⁴ | Jaerak Chang^{1,5} | Dong-Wan Kim²

¹Department of Brain Science, Ajou University School of Medicine, Suwon, Republic of Korea

²School of Civil, Environmental, and Architectural Engineering, Korea University, Seoul, Republic of Korea

³Seoul Center, Korea Basic Science Institute, Seoul, Republic of Korea

⁴Department of Chemical Engineering, Kwangju University, Seoul, Republic of Korea

⁵Department of Biomedical Sciences, Ajou University Graduate School of Medicine, Suwon, Republic of Korea

Correspondence

Dr. Eun-Jung Park, Department of Brain Science, Ajou University School of Medicine, 164, World cup-ro, Youngtong-gu, Suwon 16499, South Korea

Email: pejtoxic@hanmail.net

Dong-Wan Kim, School of Civil, Environmental, and Architectural Engineering, Korea University, Seoul, Republic of Korea
Email: dwkim1@korea.ac.kr

Funding information

R&D Center for Valuable Recycling (Global-Top R&BD Program) of the Ministry of Environment, Grant/Award Number: Project No.: R2-17_2016002250005; National Research Foundation of Korea funded by the Ministry of Education, Science and Technology, Grant/Award Number: 2011-35B-E00011

Abstract

The tissue distribution and toxicity of nanoparticles (NPs) depend on their physical and chemical properties both in the manufactured condition and within the biological system. We characterized three types of commercially available aluminum-based NPs (Al-NPs), two rod-type aluminum oxide NPs (Al_2O_3 , AIONPs), with different aspect ratios (short [S]- and long [L]-AIONPs), and spherical aluminum cerium oxide NPs (AlCeO_3 , AlCeONPs). The surface area was in order of the S-AIONPs > L-AIONPs > AlCeONPs. Very importantly, we found that AlCeONPs is Al_2O_3 -coated CeO_2 NPs, but not AlCeO_3 NPs, and that the Al level in AlCeONPs is approximately 20% of those in S- and L-AIONPs. All three types of Al-NPs were slightly ionized in gastric fluid and rapidly particlized in the intestinal fluid. There were no significant differences in the body weight gain following 28 days of repeated oral administration of the three different types of Al-NPs. All Al-NPs elevated Al level in the heart, spleen, kidney and blood at 24 hours after the final dose, accompanied by the altered tissue level of redox reaction-related trace elements. Subsequently, in four types of cells derived from the organs which Al-NPs are accumulated, H9C2 (heart), HEK-293 (kidney), splenocytes and RAW264.7 (blood), S-AIONPs showed a very low uptake level and did not exert significant cytotoxicity. Meanwhile, cytotoxicity and uptake level were the most remarkable in cells treated with AlCeONPs. In conclusion, we suggest that the physicochemical properties of NPs should be examined in detail before the release into the market to prevent unexpected adverse health effects.

KEYWORDS

aluminum oxide nanoparticles, cerium oxide nanoparticles, physicochemical properties, tissue distribution, toxicity

1 | INTRODUCTION

Owing to their great potential benefits, the market size of nanoparticle (NP)-based products has rapidly grown. However, strictly speaking, nanotoxicity research has failed in keeping pace with the development of novel NPs due to the surprising growth of the nanotechnology industry, thus numerous NP-based products have been brought to market without thorough consideration to the possible adverse effects on the environment and human health. For example, the production of metal oxide NPs is forecasted to increase from 270 041 tons in 2012

to 1663, 168 tons by 2020 (Pakrashi, Dalai, Humayun, et al., 2013). In 2010, the OECD Working Party on Manufactured Nanomaterials published a list of priority nanomaterials for toxicity testing including eight species of metal oxide NPs, which were chosen after considering their global market size, and further collected and produced their toxicity data under a worldwide cooperation. However, information on their possible adverse effects is still not sufficient.

Aluminum is one of the most abundant elements in the Earth's crust, thus humans can be frequently exposed to aluminum through food, water and air (Willhite et al., 2014). In addition, aluminum oxide NPs (Al_2O_3 , AIONPs) have been recently reported as an emerging material because of their promising technological applications. For

[†]These authors contributed equally to this work.

example, AlONPs are added into solid rocket fuel, owing to their highly effective catalytic activity, and into the sintering processes of ceramics, owing to the large surface and superficial atom ratio. They are also used for drug delivery, for preparation of nanocomposites, and as wear-resistant additives (Prabhakar et al., 2012).

Most aluminum-containing compounds have a low solubility in water, and are not easily ionized, even in acidic conditions, such as gastric juice (pH 1.5–3.5) and the lysosomal lumen (pH 4.5–5.0) (Doshi, Braida, Christodoulatos, Wazne, & O'Connor, 2008; Zhang et al., 2013). Additionally, it is known that the toxicity of NPs depends on their properties both in the manufactured condition (primary) and within a biological system (secondary) (Karunakaran, Suriyaprabha, Rajendran, & Kannan, 2015; Radziun et al., 2011). However, knowledge regarding the relationship between the properties of AlONPs and their biodistribution is extremely limited. In our previous study, we suggested that the accumulation and toxicity of rod-type AlONPs depend on the aspect ratio and surface area (Park, Lee, et al., 2015; Park, Kim, et al., 2016), and that the distribution and toxicity of spherical AlONPs are raised by the presence of the hydroxyl group due to their low stability within biological systems (Park, Lee, et al., 2016). Moreover, when exposed to macrophages, oxide-coated Al-NPs (50, 80 and 120 nm) induced greater toxicity and more clearly decreased phagocytic ability compared to AlONPs (30 and 40 nm) (Wagner et al., 2007). In the present study, we aimed to explore the effects of physical and chemical factors on both biodistribution and the biological response following the 28 day repeated oral administration of Al-NPs. Thus, we used three types of commercially available Al-NPs, two rod-type AlONPs (hereafter, short (S)- and long (L)-AlONPs; Park, Sim, et al., 2015) and aluminum cerium oxide NPs (AlCeO₃, hereafter, AlCeONPs). We also identified the tissue distribution and their effects on redox reaction-related trace elements. Additionally, we compared the cellular uptake level and in vitro toxicity of the Al-NPs using cells derived from the relevant target organs.

2 | MATERIALS AND METHODS

2.1 | Sample preparation and characterization

S- and L-AlONPs and AlCeONPs were purchased from Sigma-Aldrich (catalog nos 718475, 544833 and 637866; St. Louis, MO, USA) and loaded in deionized water at a concentration of 1 mg ml⁻¹. As described previously (Park, Lee, et al., 2015; Park, Sim, et al., 2015; Park, Kim, et al., 2016), each sample was dispersed in a stable fashion by sonication twice for 10 minutes in a bath-type sonicator (150 W, 40 kHz). The temperature of the sonicator was maintained below 30°C to prevent agglomeration between the particles. The chemical and physical characterization of all samples was investigated by using X-ray powder diffraction (XRD; model D/max-2500 V/PC; Rigaku Co., Tokyo, Japan) and transmission electron microscopy with energy dispersive X-ray spectroscopy (transmission electron microscopy [TEM] with energy-dispersive spectroscopy [EDS], Tecnai G2 F30 S-Twin; FEI, Hillsboro, OR, USA). The surface area of the samples was estimated by using a Brunauer–Emmett–Teller surface-area analyzer (BET, Belsorp mini II; BEL Japan Inc., Osaka, Japan).

2.2 | Fate analysis of administered aluminum nanoparticles

The three types of Al-NP solutions (2 ml) were diluted in artificial gastric juice (pH 2, 48 ml; Marques, Loebenberg, & Almkainzi, 2011) and maintained for a designated time at 37°C. An aliquot of the solution was transferred to another tube and centrifuged at 10274 × g for 10 minutes. The supernatant containing ionized Al (Al³⁺), was transferred into the artificial intestinal juice (pH 6.8) and incubated for a designated time at 37°C. After stirring for 30 minutes, the aggregated (or reduced) Al particles were separated by centrifugation (10274 × g for 10 minutes). The ionization level of the three types of Al-NPs in the gastric juice was measured by inductively coupled plasma (ICP) optically emitting spectra (Optima 2000DV; PerkinElmer, MA, USA) and the particulation degree in the intestinal juice was calculated from the Al ion (Al³⁺) level remaining in the intestinal juice after incubation.

2.3 | Housing and aluminum nanoparticles treatment

Six-week-old male ICR mice (26–28 g, specific pathogen free; OrientBio, Seongnam, Korea) were acclimatized in our specific pathogen-free facility (temperature, 23 ± 3°C; relative humidity, 50 ± 10%; 12 hour light/dark cycle [150–300 Lux]; and ventilation, 10–20 times per hour) for 1 week before the experiment was commenced. Access to water and food were permitted ad libitum. Considering that the no observed adverse effect level for repeated oral dosing may be lower than 6 mg kg⁻¹ (Park, Sim, et al., 2015), the Al-NPs were dosed daily by gavage (2 and 6 mg kg⁻¹, 6 days week⁻¹, 6 mice per group) for 28 days, and the control group was treated with sterilized drinking water. The experiments were conducted in accordance with OECD test guideline (no. 407) and body weight was weekly measured. The experiments (IACUC no. 2014-0021) were assessed by the Institutional Animal Care and Committee (IACUC) of Ajou University (Suwon, Korea) and performed in accordance with the ILAR publication, "Guide for the Care and Use of Laboratory Animals."

2.4 | Measurement of elemental concentrations

The tissues (brain, thymus, lung, heart, liver, spleen, kidney, testis and whole blood) were collected after parturition. As described previously (Park, Sim, et al., 2015), Al-NPs, the tissues and blood (100 µl) were digested in a mixture of 70% HNO₃ and 35% H₂O₂ using a microwave digestion system (Milestone, Sorisole, Italy) at high temperatures (120°C, 8 minutes; 50°C, 2 minutes; 180°C, 10 minutes) and high pressure. Finally, elemental concentrations in samples (Al, Cu, Zn, Mn and Fe) were measured in accordance with a standard operating procedure using ICP mass spectrometry (ICP-MS) at the Korean Basic Science Institute (Supporting information, Table S1; Seoul, Korea).

2.5 | Hematological analysis

Blood (six mice per group, approximately 1.0 ml per mouse) was taken from the caudal vena cava, and hematological analysis of the whole blood was conducted in the Neodin Veterinary Science Institute (Seoul, Korea) using a blood autoanalyzer (HemaVet850; CDC Technologies, Inc. OH, USA).

2.6 | Cellular uptake

Considering that the side-scattered light (SSC) and forward scatter axes in the fluorescence-activated cell sorter (FACS) system indicate cellular complexity (cellular uptake of NPs) and cell size, respectively, we performed FACS analysis using four types of cells derived from the target organ for accumulation of Al-NPs. The spleen was kindly provided by Prof. S. Yang (Ajou University, Seoul, Korea), and splenocytes were obtained through a previously described procedure (Park, Kim, et al., 2016). Additionally, H9C2 cells (rat cardiomyocytes), HEK-293 cells (human embryonic kidney cells) and RAW264.7 cells (murine peritoneal macrophage cells) were purchased from the Korean Cell Line Bank (Seoul, Korea). Briefly, cells (2×10^5 per well) were seeded in a 12-well plate and incubated with or without Al-NPs ($20 \mu\text{g ml}^{-1}$) for 24 h. The cells were washed with phosphate-buffered saline and resuspended in Annexin V binding buffer (Biolegend, San Diego, CA, USA). According to the manufacturer's instructions, Annexin V and propidium iodide solutions were added, incubated for 15 minutes at room temperature, and analyzed using a FACSCalibur system and CellQuest software (BD Biosciences, Franklin Lakes, NJ, USA). In addition, cells (5×10^3) were stabilized overnight in 12-well plates and incubated with or without Al-NPs ($20 \mu\text{g ml}^{-1}$) for 24 hours. Phase contrast images were obtained using a confocal microscopy (IX83; OLYMPUS, Shinjuku, Tokyo, Japan).

2.7 | Cytotoxicity test

We used a trypan blue exclusion staining method to evaluate toxicity following uptake of three types of Al-NPs at a cell level. Briefly, cells (2×10^5 cells per well) were incubated in a 12-well plate, with or without Al-NPs ($20 \mu\text{g ml}^{-1}$), for 24 hours. Cell suspension and trypan blue (Life Technologies, Grand Island, NY, USA) were mixed (1:1) and then analyzed using an automated cell counter (Countess II; Life Technologies).

2.8 | Statistical analysis

The results were presented as the mean \pm standard deviation. The statistical significance of the differences between the treated-group and the control group was assessed by using Student's *t*-test and one-way ANOVA followed by Tukey's post-hoc pairwise comparison (GraphPad Software, San Diego, CA, USA).

3 | RESULTS

3.1 | Characterization of Al-NPs

The morphologies of three types of Al-NPs were investigated using typical TEM (Figure 1A–C). S-AlONPs were well dispersed (Figure 1A),

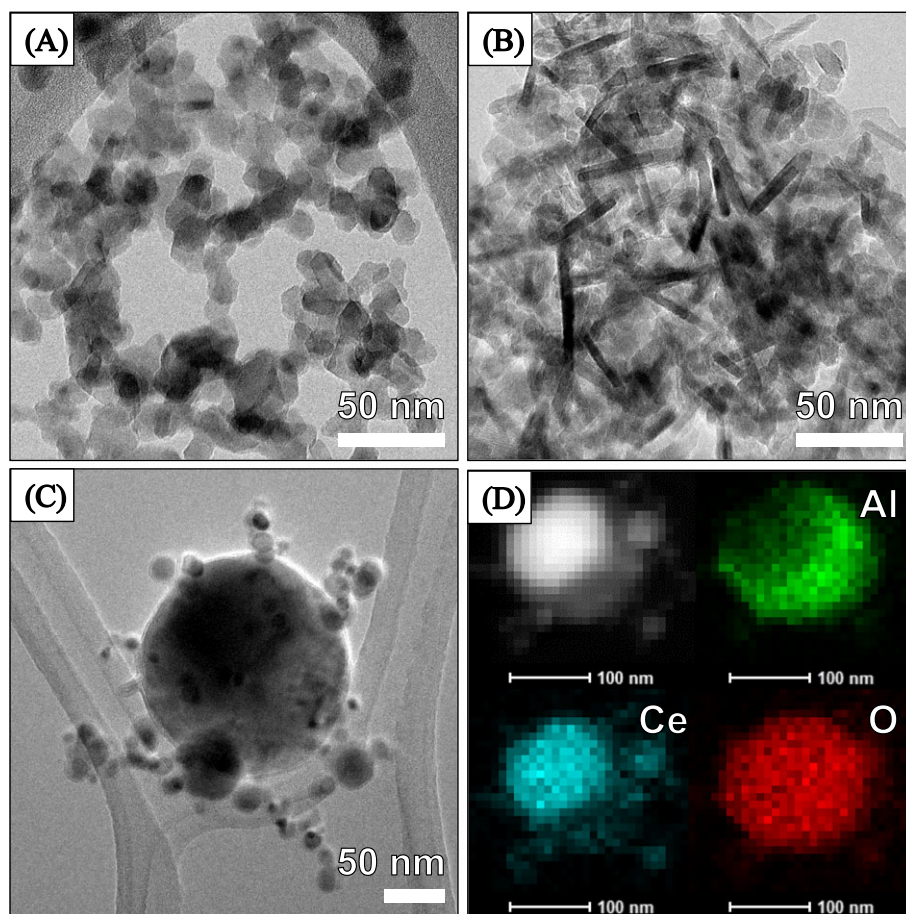


FIGURE 1 Morphological properties of Al-NPs. Typical field emission scanning electron microscopy images of (A) S- and (B) L-AlONPs and (C) AlCeONPs. (D) energy-dispersive spectroscopy mapping profile of Al, Ce and O in AlCeONPs. Al-NPs, aluminum nanoparticles; AlCeONPs, aluminum cerium oxide nanoparticles; L-AlONPs, long aluminum oxide nanoparticles; S-AlONPs, short aluminum oxide nanoparticles

whereas L-AIONPs showed an aggregated appearance (Figure 1B). S- and L-AIONPs had anisotropic shapes with different aspect ratios (length-to-diameter) of 2.1 ± 0.4 , and 6.2 ± 0.6 , respectively (Park, Lee, et al., 2015; Park, Kim, et al., 2016). The XRD patterns obtained from both S- and L-AIONPs were primarily indexed to δ phase, although S-AIONPs were δ phase with the I space group (PDF no. 00-016-0394; $a = b = 7.94 \text{ \AA}$, $c = 23.50 \text{ \AA}$, $\alpha = \beta = \gamma = 90^\circ$, volume = 1482.6 \AA^3), and L-AIONPs were δ phase with the $P-4m2$ space group (PDF no. 00-046-1131; $a = b = 5.60 \text{ \AA}$, $c = 23.66 \text{ \AA}$, $\alpha = \beta = \gamma = 90^\circ$, volume = 741.6 \AA^3) (Supporting information, Figure S1A and B). AlCeONPs were estimated to have a large sphere with a diameter of approximately 150 nm that surrounded small spheres with heterogeneous diameters (Figure 1C). The XRD patterns obtained from AlCeONPs were primarily indexed to CeO_2 (PDF no. 00-004-0593) and to weak peaks of $\gamma\text{-Al}_2\text{O}_3$ (PDF no. 10-0425) (Supporting information, Figure S1C). Subsequently, the chemical composition of AlCeONPs was investigated using a high-angle annular dark-field scanning TEM equipped with an EDS apparatus. The EDS mapping profile of AlCeONPs, shown in Figure 1(D), clearly indicated that the outer sheath was composed of Al_2O_3 and CeO_2 was present in the inner part of the NP. Furthermore, the Al content in AlCeONPs was approximately 20.0% and 21.9% of that in S- and L-AIONPs, respectively (Table 1). Therefore, we concluded that AlCeONPs are Al_2O_3 -coated CeO_2 NPs, rather than AlCeO_3 NPs, although it is selling under the trade name "AlCeO₃." In addition, the BET specific surface areas of S- and L-AIONPs and AlCeONPs from the N_2 adsorption-desorption isotherms at room temperature were 163.4, 105.9 and $24.8 \text{ m}^2 \text{ g}^{-1}$, respectively (Supporting information, Figure S2).

3.2 | Fate of Al-NPs in the body fluid

To monitor the fate of Al-NPs within the biological system, we evaluated the ionization degree of Al-NPs in gastric juice and their particlization level in the intestinal juice. The ionization ratio (C/C_0) of the Al-NPs in gastric juice (pH 2) was slightly increased with time (Figure 2A). Meanwhile, the ionization level (C/C_0 , conversion yield of Al^{3+} from Al-NPs; C_0 for initial concentration of Al) was slightly different by types of Al-NPs (AlCeONPs > L-AIONPs > S-AIONPs, approximately 2–13%, regardless of the types of Al-NPs; Figure 2A). Additionally, in the intestinal juice (pH 6.8), Al particles were reformed from the three types of ionic solution and the particlization level was close to 90% in all three types of Al-NPs after 24 hour incubation (Figure 2B). In addition, if some NPs have high acid resistance, particles might have good stability and dispersity in acidic solutions. In this study, Al-NPs dispersed in drinking water exhibited intrinsic surface properties (surface charge) and behavior (hydrodynamic diameter,

HDD) in the liquid phase (Table 2). HDD of S-AIONPs dispersed in drinking water was smaller than that of L-AIONPs, but the surface charge was similar between them (<10 mV). AlCeONPs with a negative charge showed a 384 nm aggregated form, similar to S-AIONPs, even though its surface area is approximately sixfold lower than S-AIONPs. When the Al-NPs were exposed to an acidic solution, such as gastric juice, the particle size of both S-AIONPs and L-AIONPs decreased due to the partial dissolution (Figure 2A) of the external surface of the AIONPs, as compared to that exposed in drinking water (i.e., $318 \rightarrow 176 \text{ nm}$; $830 \rightarrow 776 \text{ nm}$). Whereas, AlCeONPs with more negative surface charge did not show a decrease of particle size after dispersion in gastric juice. Namely, good dispersion stability in acidic solution is due to the interparticle repulsion induced by high negative surface charge. As intestinal juice has neutral pH condition, the Al-NPs dispersed in this solution have a similar HDD with that in drinking water. The surface charge of all Al-NPs exposed to intestinal juice was shifted to a more positive value. The various organic compounds contained in artificial intestinal juice (enzyme, protein, salts, etc.) were induced the protein-corona effect and thus the surface charge of particles changed to more positive charge.

3.3 | Effects on body weight changes

Although the changes were not statistically significant, the body weight gain of mice tended to be lower in the group administered with the higher dose of Al-NPs compared to that in the control group (Table 3; Supporting information, Figure S3). That is, the body weight of mice in the control group was 29.6 ± 0.7 and $35.8 \pm 1.2 \text{ g}$ at days 0 and 28, respectively, whereas the body weight in the higher dose of S-AIONP-, L-AIONP- and AlCeONP-treated mice was 30.1 ± 0.8 , 30.0 ± 0.6 and $30.1 \pm 0.9 \text{ g}$, respectively, at day 0, and 35.4 ± 1.1 , 35.8 ± 0.7 and $35.5 \pm 2.3 \text{ g}$, respectively, at day 28. Therefore, it was calculated that the average body weight gain is 5.28, 5.88 and 5.37 g, in the higher dose groups of S-AIONPs, L-AIONPs and AlCeONPs, respectively, and 6.2 g in the control group.

3.4 | Tissue distribution of Al-NPs

Dose-related increase in the tissue Al level following repeated administration of Al-NPs were observed in the kidney, spleen and blood. Additionally, when comparing the higher dose (6 mg kg^{-1}) of Al-NP-treated groups and the control group, Al level in the heart, kidney, spleen and blood was significantly increased by the three types of Al-NPs (Table 4). There was no significant increase in Al from brain, liver, thymus testis and lung when comparing the 6 mg kg^{-1} dose to the control group. Furthermore, S- and L-AIONPs raised the Al level in the thymus, and S-AIONPs and AlCeONPs increased the Al level in the brain.

3.5 | Effects on redox reaction-related elements in tissues

Considering that AIONPs induced toxicity via oxidative stress, we investigated effects of the Al-NPs on redox reaction-related elements in tissues (Alarifi, Ali, & Alkahtani, 2015; Alshatwi et al., 2013; Shah et al., 2015; Shrivastava, Raza, Yadav, Kushwaha, & Flora, 2014;

TABLE 1 Comparison of Al content in Al-NPs

	Al ($\mu\text{g ml}^{-1}$)	Ce ($\mu\text{g ml}^{-1}$)
S-AIONPs	657 775	–
L-AIONPs	602 767	–
AlCeONPs	131 867	604 057

AlCeONPs, aluminum cerium oxide nanoparticles; L-AIONPs, long aluminum oxide nanoparticles; S-AIONPs, short aluminum oxide nanoparticles.

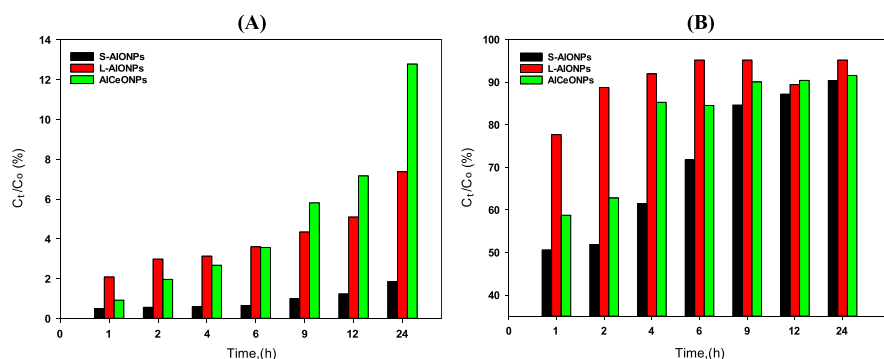


FIGURE 2 Fate of Al-NPs in biological fluids. Three types of Al-NPs were loaded into artificial gastric juice at $100 \mu\text{g ml}^{-1}$. (A) Ionization rate of Al-NPs in artificial gastric juice. (B) Particulation rate in artificial intestinal juice. Al-NPs, aluminum nanoparticles; AlCeONPs, aluminum cerium oxide nanoparticles; L-AIONPs, long aluminum oxide nanoparticles; S-AIONPs, short aluminum oxide nanoparticles.

Srikanth, Mahajan, Pereira, Duarte, & Venkateswara Rao, 2015). Dose-related changes in the level of redox reaction-related elements following the increase of the tissue Al level were not remarkable. Meanwhile, when comparing the higher dose of Al-NP-treated groups and the control group, Mn and Fe level significantly increased in the liver of all the treated groups (Table 5). Mn level also decreased in the brain of all the treated groups and Fe level was clearly elevated in the spleen in S- and L-AIONP-treated groups. Cu level notably increased in the liver in mice exposed to S- and L-AIONPs and in the kidney in mice exposed to S-AIONPs and AlCeONPs. Additionally, Zn level was clearly raised in the kidney in all the treated groups and in the spleen in the AlCeONP-treated group. Meanwhile, Cu and Zn levels markedly decreased in the thymus and the testis, respectively, in all the treated groups, and S-AIONPs clearly increased Cu and Zn levels in the blood.

3.6 | Effects on blood hematology

After the 28 day repeated oral administration, the higher dose of S- and L-AIONPs significantly increased the number of white blood cells (WBC) compared to the control (2.0- and 1.9-fold, respectively), and the higher dose of S-AIONPs elevated the monocyte portion in WBC (approximately 1.5-fold; Table 6). However, there were no significant hematological changes in the blood of mice exposed to AlCeONPs.

3.7 | Effects on cellular uptake and cytotoxicity

To predict the toxic level following bioaccumulation of the three different types of Al-NPs, we used four types of cells derived from the

TABLE 2 Summary of the properties of Al-NPs in biological fluids. Data are the mean \pm SD of three independent measurements

		Hydrodynamic diameter (nm)	Surface charge (mV)
Drinking water	S-AIONPs	318.6 ± 11.6	9.9 ± 0.4
	L-AIONPs	830.2 ± 16.6	5.5 ± 0.4
	AlCeONPs	384.2 ± 14.3	-10.3 ± 0.7
Gastric juice	S-AIONPs	175.9 ± 10.6	-23.7 ± 0.9
	L-AIONPs	776.1 ± 11.2	40.8 ± 1.0
	AlCeONPs	386.4 ± 17.4	-21.6 ± 0.7
Intestinal juice	S-AIONPs	272.4 ± 16.5	33.5 ± 0.4
	L-AIONPs	867.4 ± 23.9	26.3 ± 0.7
	AlCeONPs	471.4 ± 23.5	10.8 ± 1.0

AlCeONPs, aluminum cerium oxide nanoparticles; L-AIONPs, long aluminum oxide nanoparticles; S-AIONPs, short aluminum oxide nanoparticles.

organs, which Al-NPs was accumulated, H9C2 (heart), HEK293 (kidney), RAW264.7 (blood) and primary splenocytes (spleen). First, considering that the SSC axis in FACS analysis indicates cellular complexity (including the cellular uptake of NPs), we performed FACS analysis after Annexin V staining with propidium iodide at 24 hours after exposure to Al-NPs ($20 \mu\text{g}/2 \times 10^5$ cells). The distribution of cells exposed to AlCeONPs was evidently shifted on the upper SSC axis in all types of cells accompanied by a decrease of cell size (Figure 3A). The marked cellular uptake of AlCeONPs was also visually confirmed (Supporting information, Figure S4). Importantly, S-AIONPs did not induce significant cytotoxicity in the four types of cells evaluated in this study (Figure 3B). On the other hand, L-AIONPs and AlCeONPs significantly inhibited the viability of all types of cells and the decreased level was clearer in AlCeONP-treated cells compared to that of L-AIONP-treated cells, which is associated with the cellular uptake level of the Al-NPs.

4 | DISCUSSION

The high stabilization of NPs within a biological system is essential for the application of NPs in medical and pharmacological fields (Lo, Kwon, Zhang, Singhal, & Bhatia, 2016; Mao, Tsai, Chen, Yan, & Wang, 2016; Utembe, Potgieter, Stefaniak, & Gulumian, 2015). However, it is well known that the properties of NPs are rapidly altered in biological fluids, thus NPs can induce different toxicity with that expected in the manufactured condition within the biological system (Higashisaka, Nagano, Yoshioka, & Tsutsumi, 2017; Nel et al., 2009). For example, in our previous study, the accumulation and toxicity of spherical AIONPs were more marked in mice exposed to γ -aluminum oxide hydroxide NPs compared with those of γ -AIONPs and α -AIONPs due to their low stability within biological systems (Park, Lee, et al., 2016), and the surface coating of Zn oxide NPs with phosphate and sulfide, which have very low solubility in water, did not attenuate tissue distribution and toxicity of Zn oxide NPs following 28 days of oral administration due to the higher particulation rate of Zn oxide NPs in the intestine (Park, Jeong, Yoon, & Kim, 2017). Additionally, the inflammatory response produced in cells exposed to AIONPs (50 and 80 nm) depended on the surface area dose instilled, but not the mass dose instilled, emphasizing the importance of media- and temperature-dependent particle agglomeration levels in assessing the biological safety of nanomaterials (Duffin, Tran, Brown, Stone, & Donaldson, 2007). Furthermore, some NPs, composed of Co, Ag and Zn, are easily

TABLE 3 Changes of body weight. Three types of Al-NPs were administered orally for 28 days (six times per week). Body weight was measured weekly after administration ($n = 6$)

	Control	S-AIONPs		L-AIONPs		AlCeONPs	
		2 mg kg ⁻¹	6 mg kg ⁻¹	2 mg kg ⁻¹	6 mg kg ⁻¹	2 mg kg ⁻¹	6 mg kg ⁻¹
Day 0	29.6 ± 0.7	29.5 ± 1.0	29.4 ± 0.8	29.5 ± 0.8	29.3 ± 0.6	29.6 ± 0.9	29.4 ± 0.9
Day 7	33.3 ± 0.7	32.2 ± 1.9	33.3 ± 1.2	33.3 ± 1.0	32.8 ± 0.7	33.3 ± 1.4	32.4 ± 1.8
Day 14	33.3 ± 0.8	33.1 ± 1.9	32.9 ± 1.3	34.1 ± 1.2	33.5 ± 0.9	33.6 ± 1.6	32.9 ± 2.1
Day 21	34.7 ± 0.9	34.3 ± 2.1	33.7 ± 1.3	35.3 ± 1.3	34.3 ± 0.8	34.5 ± 1.4	33.9 ± 2.5
Day 28	35.8 ± 1.2	35.2 ± 2.3	34.7 ± 1.1	36.9 ± 1.6	35.2 ± 0.7	35.3 ± 1.3	34.8 ± 2.3

AlCeONPs, aluminum cerium oxide nanoparticles; L-AIONPs, long aluminum oxide nanoparticles; S-AIONPs, short aluminum oxide nanoparticles.

dissolved in biological fluids and induce greater toxicity than that observed in the particulate state, and Fe oxide NPs are easily oxidized within biological systems, which results in the production of more radicals and followed by stronger toxicity. Therefore, both the properties in the manufactured condition (primary) and the properties within the biological system (secondary) must be carefully considered in the interpretation of toxicity test results. First, shape and surface area are among the key factors in the determination of the toxicity of nano-sized particles (Bakand, Hayes, & Dechsakulthom, 2012; Fröhlich & Roblegg, 2016; Li et al., 2015). In the current study, S- (2.1 ± 0.4) and L-AIONPs (6.2 ± 0.6) were rod-shaped, which have different aspect ratios (Park, Lee, et al., 2015), and AlCeONPs were spherical, which can flow more easily in the bloodstream compared to the two rod types of AIONPs. The surface area, which was in the order S-AIONPs > L-AIONPs > AlCeONPs, was approximately 6.6- and 4.3-fold greater in S- and L-AIONPs, respectively, compared with that of AlCeONPs. The dissolution rate was also an important factor in nanotoxicity. The three types of Al-NPs used in this study are known to have poor solubility in the water phase (<https://www.sciencelab.com/msds.php?msdsId=9922858>), and owing to the very strong bonding between the aluminum and oxygen ions, there is a lack of space for water molecule penetration. However, these particles could react with both acids and bases to form salts (Franke, Ernst, & Myerson, 1987; Pakrashi, Dalai, Prathna, et al., 2013) and could be dispersed in various ionic solutions (Cherginets et al., 2006). In the present study, the three types of Al-NPs showed a relatively low ionization rate in gastric juice, in

particular, S-AIONPs were not ionized for 24 hours. Additionally, the given data showed that the Al level in tissue after 28 days of oral dosing was not significantly different among the three types of Al-NPs. Al₂O₃ and CeO₂ are insoluble in water. The molecular weight of AlCeO₃ is 215.10 with one Al ion in a molecule, and that of Al₂O₃ is 101.96 with two Al ions in a molecule. Therefore, the Al content in 1 mol AlCeO₃ and Al₂O₃ is 12.5% and 52.9%, respectively, and this computation was confirmed by ICP-MS analysis. Thus, we can anticipate that if the three types of Al-NPs were administered at the same mass dose, the Al level resulting from S- and L-AIONPs may be approximately 4.2-fold greater than that of AlCeONPs. More importantly, in our previous studies, L-AIONPs were distributed in the liver, kidney, lung and heart, but not the brain, after repeated oral dosing for 90 days (Park, Sim, et al., 2015), and sphere-type AIONPs accumulated in the brain, thymus and lung, but not the liver, after repeated oral dosing for 28 days (Park, Kim, Kim, & Choi, 2011). In the current study, AlCeONPs (sphere-type), but not S- and L-AIONPs, elevated the Al level in the brain after the 28 day oral administration; it also surrounded the nuclear membrane of cells, with more evident cellular uptake compared to the other two AIONPs at 24 hours exposure. Therefore, we hypothesize that the bio-accumulation of AlCeONPs may be more noticeable compared with that of S- and L-AIONPs. Considering that alumina has been proposed as an inducer of Alzheimer's disease (Ferreira, Piai Kde, Takayanagi, & Segura-Muñoz, 2008) and that AlCeONPs have shown neuroprotective effects (Arya et al., 2016; Bailey et al., 2016; Najafi, Hosseini, Ghaznavi, Mehrzadi, & Sharifi, 2017), we also suggest that further study

TABLE 4 Al level in tissues. Tissue and blood ($n = 6$) were harvested at 24 hours after the final dose and digested in a mixed solution of 70% HNO₃ (7 ml) and 35% H₂O₂ solution (1 ml). Two lysates were pooled to produce one sample for analysis ($n = 3$)

Al	Control	S-AIONPs		L-AIONPs		AlCeONPs	
		2 mg kg ⁻¹	6 mg kg ⁻¹	2 mg kg ⁻¹	6 mg kg ⁻¹	2 mg kg ⁻¹	6 mg kg ⁻¹
Brain	1403.8 ± 181.9	1644.9 ± 150.3	1678.1 ± 314.5	1519.2 ± 272.6	1548.8 ± 328.8	1807.3 ± 281.4 [†]	1958.0 ± 263.0**
Heart	4001.4 ± 1254.8	6982.0 ± 734.5**	9363.1 ± 771.2**	8284.9 ± 855.3**	8293.6 ± 3519.0	8936.2 ± 3070.3**	10296.9 ± 2594.7**
Liver	1046.4 ± 161.6	1041.4 ± 134.4	1207.2 ± 78.6	1404.1 ± 297.8	1897.2 ± 1210.7	919.4 ± 102.5	1207.3 ± 56.1
Thymus	4683.7 ± 653.3	4581.3 ± 1106.5	6580.1 ± 1136.6**	5747.7 ± 866.9	7871.4 ± 1524.8**	4342.1 ± 649.7	5604.4 ± 369.2 [†]
Kidney	2135.9 ± 439.7	3125.2 ± 309.7**	4130.8 ± 1167.7**	2418.3 ± 165.6	3925.4 ± 287.4**	3495.6 ± 561.7**	3669.6 ± 929.1**
Testis	2432.5 ± 307.4	2126.0 ± 173.6	2643.3 ± 757.8	2588.2 ± 781.1	2847.5 ± 190.9	2391.7 ± 106.1	2657.4 ± 303.6
Lung	2279.9 ± 398.7	2179.6 ± 154.9	2783.8 ± 756.2	2074.8 ± 34.5	2250.4 ± 119.7	2196.9 ± 490.9	2983.9 ± 371.9 [†]
Spleen	3418.2 ± 299.1	3484.1 ± 583.2	4758.8 ± 925.5**	4014.1 ± 900.7	7176.2 ± 2079.4**	4077.2 ± 182.5**	6610.5 ± 2293.3**
Blood	780.1 ± 100.9	2044.5 ± 330.8**	3225.6 ± 404.6**	1150.7 ± 213.0**	1383.5 ± 279.8**	1411.0 ± 300.9**	1511.6 ± 145.4**

AlCeONPs, aluminum cerium oxide nanoparticles; L-AIONPs, long aluminum oxide nanoparticles; S-AIONPs, short aluminum oxide nanoparticles.

Results represent the mean ± SD.

**P < 0.01.

TABLE 5 Tissue level of redox reaction-related trace elements. Results represent the mean \pm SD (n = 3)

	S-AIONPs			L-AIONPs			AICeONPs		
	Control	2 mg kg ⁻¹	6 mg kg ⁻¹	2 mg kg ⁻¹	6 mg kg ⁻¹	6 mg kg ⁻¹	2 mg kg ⁻¹	6 mg kg ⁻¹	6 mg kg ⁻¹
Mn									
Brain	471.1 \pm 38.6	404.3 \pm 15.3**	428.9 \pm 18.9*	399.2 \pm 19.0**	410.7 \pm 2.7**	408.0 \pm 27.9**	389.0 \pm 15.3**	408.0 \pm 27.9**	408.0 \pm 27.9**
Heart	716.4 \pm 106.9	667.4 \pm 47.1	707.7 \pm 47.4	731.7 \pm 62.2	744.7 \pm 9.6	765.2 \pm 71.1	705.9 \pm 102.0	765.2 \pm 71.1	765.2 \pm 71.1
Liver	936.4 \pm 30.9	1093.1 \pm 105.9*	1175.9 \pm 16.7**	1057.5 \pm 80.8*	1081.8 \pm 59.4**	1041.3 \pm 28.7**	909.5 \pm 86.7	1041.3 \pm 28.7**	1041.3 \pm 28.7**
Thymus	302.5 \pm 23.6	332.5 \pm 46.5	263.1 \pm 17.0	296.0 \pm 3.1	340.9 \pm 28.1*	308.4 \pm 21.6	285.8 \pm 38.4	308.4 \pm 21.6	308.4 \pm 21.6
Kidney	1779.8 \pm 1230	1906.3 \pm 108.3	1997.5 \pm 89.4*	1929.4 \pm 186.0	2142.6 \pm 291.2	1989.7 \pm 166.7	1901.3 \pm 37.6	1989.7 \pm 166.7	1989.7 \pm 166.7
Testis	601.9 \pm 140.1	645.7 \pm 110.5	479.3 \pm 60*	469.6 \pm 9.4*	469.8 \pm 24.7	532.4 \pm 64.6	490.9 \pm 17.6	532.4 \pm 64.6	532.4 \pm 64.6
Lung	240.5 \pm 1.4	243.9 \pm 37.1	267.2 \pm 64.0	236.2 \pm 28.1	271.2 \pm 25.8*	244.0 \pm 11.2*	198.9 \pm 11.3	244.0 \pm 11.2*	244.0 \pm 11.2*
Spleen	304.9 \pm 22.6	281.2 \pm 33.2	353.8 \pm 76.2	302.9 \pm 120.4	287.3 \pm 35.1	317.4 \pm 19.0	253.4 \pm 16.9	317.4 \pm 19.0	317.4 \pm 19.0
Blood	ND	ND	ND	ND	ND	ND	ND	ND	ND
Cu									
Brain	3221.9 \pm 1900	3188.8 \pm 160.4	3482.2 \pm 166.8	3272.5 \pm 75.3	3347.9 \pm 145.7	3521.3 \pm 279.9	3327.3 \pm 158.3	3521.3 \pm 279.9	3521.3 \pm 279.9
Heart	5790.8 \pm 441.4	5673.3 \pm 470.7	5839.9 \pm 374.7	6330.6 \pm 124.5*	5627.5 \pm 37.4	5698.7 \pm 647.2	6095.8 \pm 38.8	5698.7 \pm 647.2	5698.7 \pm 647.2
Liver	4028.6 \pm 222.1	4900.7 \pm 350.0**	5235.0 \pm 438.9**	4603.4 \pm 509.2	4849.0 \pm 246.8**	4523.4 \pm 546.2	4094.4 \pm 75.3	4523.4 \pm 546.2	4523.4 \pm 546.2
Thymus	1195.8 \pm 66.9	1319.6 \pm 346.6	882.6 \pm 57.4**	1129.9 \pm 53.0	951.6 \pm 43.5**	903.6 \pm 77.7**	1180.3 \pm 115.3	903.6 \pm 77.7**	903.6 \pm 77.7**
Kidney	4067.6 \pm 199.3	4323.4 \pm 220.3	4505.9 \pm 87.3**	4417.9 \pm 282.2	4431.0 \pm 179.6*	4505.3 \pm 154.8**	4324.7 \pm 291.2	4505.3 \pm 154.8**	4505.3 \pm 154.8**
Testis	1281.2 \pm 37.6	1180.2 \pm 5.7**	1135.1 \pm 14.1**	1177.2 \pm 13.5**	1057.5 \pm 16.3**	1181.4 \pm 35.5**	1282.9 \pm 97.9	1181.4 \pm 35.5**	1181.4 \pm 35.5**
Lung	2499.7 \pm 153.7	2273.3 \pm 54.1*	2263.8 \pm 83.9*	2336.3 \pm 216.5	2493.2 \pm 320.6	2386.7 \pm 161.7	2388.8 \pm 72.4	2386.7 \pm 161.7	2386.7 \pm 161.7
Spleen	1141.8 \pm 45.6	1244.8 \pm 65.4*	1079.1 \pm 45.2*	1115.3 \pm 96.6	1148.2 \pm 61.2	1260.0 \pm 128.2	1015.8 \pm 27.2**	1260.0 \pm 128.2	1260.0 \pm 128.2
Blood	549.2 \pm 31.5	637.1 \pm 53.8*	714.4 \pm 16.5**	551.1 \pm 16.3	578.0 \pm 19.5	552.0 \pm 13.3	557.3 \pm 25.8	552.0 \pm 13.3	552.0 \pm 13.3
Zn									
Brain	14 587.1 \pm 274.4	13 205.0 \pm 312.5**	13 820.6 \pm 493.2	13 857.9 \pm 279.9	13 966.0 \pm 415.6	14 123.4 \pm 667.5	13 846.8 \pm 220.3	14 123.4 \pm 667.5	14 123.4 \pm 667.5
Heart	21 692.0 \pm 2766.6	20 824.1 \pm 2641.5	22 315.6 \pm 344.2	20 954.6 \pm 118.6	22 728.6 \pm 901.4	23 108.7 \pm 1824.7	22 212.0 \pm 844.1	23 108.7 \pm 1824.7	23 108.7 \pm 1824.7
Liver	26 307.6 \pm 1603.2	26 785.9 \pm 611.0	27 141.6 \pm 1155.8	27 566.1 \pm 1610.1	27 018.9 \pm 1326.4	26 150.8 \pm 787.9	25 861.2 \pm 1433.7	26 150.8 \pm 787.9	26 150.8 \pm 787.9
Thymus	20 040.0 \pm 789.1	20 099.0 \pm 2362.5	21 484.0 \pm 599.4	20 808.8 \pm 666.8	19 842.4 \pm 694.5	19 808.2 \pm 1868.0	20 190.8 \pm 1177.0	19 808.2 \pm 1868.0	19 808.2 \pm 1868.0
Kidney	20 026.6 \pm 1129.4	22 180.1 \pm 1557.3	24 079.6 \pm 1000.0***	22 358.9 \pm 951.6*	22 639.5 \pm 717.6**	23 171.4 \pm 1050.9**	22 501.5 \pm 1094.3*	23 171.4 \pm 1050.9**	23 171.4 \pm 1050.9**
Testis	22 954.9 \pm 1390.0	20 938.9 \pm 347.4**	21 100.8 \pm 146.2**	21 186.9 \pm 332.5*	20 600.7 \pm 14.0**	20 902.9 \pm 285.2**	21 518.8 \pm 808.0	20 902.9 \pm 285.2**	20 902.9 \pm 285.2**
Lung	17 754.8 \pm 951.4	16 934.8 \pm 168.3	17 490.7 \pm 605.6	16 973.4 \pm 634.9	17 185.3 \pm 703.9	18 130.3 \pm 314.3	16 907.2 \pm 657.8	18 130.3 \pm 314.3	18 130.3 \pm 314.3
Spleen	22 468.1 \pm 505.6	21 926.4 \pm 1496.8	23 751.3 \pm 671.8**	21 197.6 \pm 389.7	22 729.3 \pm 262.6	25 017.6 \pm 951.4**	21 542.6 \pm 213.3	25 017.6 \pm 951.4**	25 017.6 \pm 951.4**
Blood	4219.6 \pm 44.5	5430.8 \pm 347.4**	7170.2 \pm 1410.0**	4833.8 \pm 72.4**	4928.4 \pm 84.0**	4907.6 \pm 75.1**	4692.1 \pm 62.5**	4907.6 \pm 75.1**	4907.6 \pm 75.1**
Fe									
Brain	20 774.6 \pm 2721.5	18 247.2 \pm 1042.5	23 854.5 \pm 3942.4	17 414.2 \pm 655.9	17 570.3 \pm 387.7	18 120.7 \pm 115.4	19 209.3 \pm 1845.1	18 120.7 \pm 115.4	18 120.7 \pm 115.4
Heart	104 487.5 \pm 12 512.7	109 789.7 \pm 15 295.4	99 048.7 \pm 5219.4	93 830.0 \pm 278.1*	98 220.8 \pm 7219.2	170 237.6 \pm 100 985.3	102 063.0 \pm 2204.8	170 237.6 \pm 100 985.3	170 237.6 \pm 100 985.3
Liver	169 449.4 \pm 12 287.1	218 926.1 \pm 9935.1**	259 746.1 \pm 31 564.4**	223 554.0 \pm 24 677.3**	226 461.2 \pm 20 116.0**	252 563.8 \pm 26 751.7**	210 015.9 \pm 8421.2**	252 563.8 \pm 26 751.7**	252 563.8 \pm 26 751.7**

(Continues)

TABLE 5 (Continued)

	S-AIONPs		L-AIONPs		AlCeONPs		
	Control	2 mg kg ⁻¹	6 mg kg ⁻¹	2 mg kg ⁻¹	6 mg kg ⁻¹	2 mg kg ⁻¹	6 mg kg ⁻¹
Thymus	51 806.9 ± 7378.7	46 168.7 ± 8991.5	63 679.4 ± 2620.3**	54 192.4 ± 4809.7	53 346.8 ± 7492.3	55 358.5 ± 6771.1	63 031.9 ± 6696.3*
Kidney	95 860.9 ± 5525.1	95 907.0 ± 2321.5	100 096.2 ± 7094.0	93 423.1 ± 5229.0	94 334.9 ± 6111.1	83 114.8 ± 2676.4	97 900.2 ± 8223.0
Testis	25 966.5 ± 1980.8	24 866.1 ± 1466.2	67 544.7 ± 32 605.6**	23 037.6 ± 1813.0	22 783.5 ± 2582.9	25 254.0 ± 1017.8	39 021.6 ± 21 858.1
Lung	119 538.4 ± 8210.7	145 174.2 ± 3428.4**	145 268.3 ± 6401.0**	136 619.5 ± 9409.8*	132 443.2 ± 10 997.7	133 114.6 ± 7116.4*	133 699.6 ± 9237.8*
Spleen	641 368.2 ± 98 593.5	631 565.8 ± 168 950.6	834 847.0 ± 37 398.7**	733 849.6 ± 42 242.8	826 012.1 ± 46 170.5**	624 528.9 ± 20 000.9	683 132.5 ± 49 856.8
Blood	480 765.3 ± 1704.1	508 512.2 ± 10 039.0**	509 418.4 ± 42 655.2	510 493.7 ± 26 795.0*	504 844.3 ± 9498.4**	493 528.3 ± 18 088.6	511 941.6 ± 22 768.1**

AlCeONPs, aluminum cerium oxide nanoparticles; L-AIONPs, long aluminum oxide nanoparticles; ND, not determined; S-AIONPs, short aluminum oxide nanoparticles.

* $P < 0.05$;

** $P < 0.01$.

is needed regarding both the morphological effects on the tissue distribution of AlCeONPs and the neurotoxicity of AlCeONPs.

In a previous study, AIONPs stimulated the antioxidant defense mechanisms (Mn-, Zn- and Cu-superoxide dismutase) via the generation of free radicals, ultimately leading to neurotoxic effects on locomotion behavior (Li et al., 2012). Similarly, aluminum-induced brain damage altered the level of antioxidant elements in the brain (Solfrizzi et al., 2006; Tripathi et al., 2009), and pulmonary exposure to AIONPs induced the inflammatory response with oxidative stress (Lu et al., 2009). Additionally, in our previous studies, AIONPs influenced the tissue homeostasis of redox reaction-related trace elements, including Mn, Zn, Cu and Fe (Park, Sim, et al., 2015; Park, Kim, et al., 2016; Park, Lee, et al., 2016). In the present study, we also found that the level of redox-reaction-related trace elements in tissues was altered after exposure to the three types of AIONPs. Moreover, compared to Mn and Fe, the Cu and Zn level in tissues appeared to be more closely associated with the accumulation of AIONPs. Although the level is extremely low, AIONPs are ionized in biological fluids. Al₂O₃ is an amphoteric oxide that can react as both an acid and a base, some metals including, Cu, Zn, Sn and Pb also form amphoteric oxides. Therefore, we hypothesize that the alteration of redox reaction-related elemental levels in tissues following the accumulation of AIONPs may be a process to remove generated reactive oxygen species or the effect of the cross-binding of the Al ion with amphoteric ions in tissues (Willhite et al., 2014).

In our previous studies, the intravenous injection of L-AIONPs (5 mg kg⁻¹) increased the portion of neutrophils and monocytes in WBC, and the repeated oral administration of L-AIONPs (6 mg kg⁻¹) for 13 weeks markedly increased the number of WBC with the decreased proportion of eosinophils. Similarly, a significant decrease in WBC, neutrophils, lymphocytes and monocytes, and a significant increase in platelets were observed after 28 days of repeated oral dosing with AIONPs (Park et al., 2011). Additionally, vanadium oxide NPs dosed orally penetrated red blood cells and accumulated in the spleen, where dead red blood cells are removed (Park, Lee, Yoon, & Kim, 2016). In the current study, three types of Al-NPs raised the Al level in the blood and spleen at 24 hours after the final dose, and S- and L-AIONPs clearly elevated the number of WBC and the proportion of monocytes. Herein, we again highlight that AIONPs may induce adverse health effects by disturbing immune function in the host. We suggest the need of further studies for the effects of AIONPs on the differentiation of hematopoietic stem cells.

Considering that toxicity tests using cultured or primary cells have been proposed as the most optimal method for the replacement of animal experiments (Radziun et al., 2011; Shrivastava et al., 2014), we assessed the cellular uptake and toxicity of three types of Al-NPs using cells derived from the organs in which Al-NPs were accumulated (heart, kidney, blood and spleen). Interestingly, at 24 hours after exposure, the uptake of AlCeONPs was more marked in all cells used in this study compared to that of S- and L-AIONPs. In a previous study, CeONPs penetrated rapidly into the human bronchial epithelial cells by the electrostatic power and located around the nucleus membrane inducing a dose-dependent cytotoxicity (Park, Choi, Park, & Park, 2008). Considering that AlCeONPs were in the form of Al₂O₃-coated CeO₂ NPs, but not AlCeO₃, we hypothesize that the intracellular fate of AlCeONPs may be similar to that of CeONPs, but not AIONPs, and that it may be due to

TABLE 6 hematological changes in the blood

	WBC K μl^{-1}	LY %	MO %	NE %	EO %	BA %	RBC M μl^{-1}	MCV fL	HCT %	MCH Pg	MCHC g dl^{-1}	Hb g dl^{-1}	RDW %	PLT K μl^{-1}	MPV fL
2 mg kg^{-1}															
Control	2.3 ± 0.6	90.6 ± 1.9	2.4 ± 0.4	5.2 ± 1.4	0.9 ± 0.6	0.6 ± 0.3	8.1 ± 0.3	53.3 ± 1.5	46.3 ± 4.8	16.5 ± 1.3	30.2 ± 2.9	14.0 ± 0.9	17.6 ± 0.5	1010.6 ± 78.5	7.3 ± 0.3
S-AIONPs	3.9 ± 1.4	88.3 ± 2.7	3.0 ± 0.4	4.9 ± 0.7	3.6 ± 1.8	0.7 ± 0.2	8.8 ± 0.2	55.1 ± 0.8	47.6 ± 2.4	15.6 ± 1.0	28.8 ± 1.4	13.4 ± 1.3	17.9 ± 0.4	868.6 ± 169.8	7.9 ± 0.7
L-AIONPs	5.1 ± 1.5	90.0 ± 2.4	2.9 ± 0.6	4.8 ± 1.2	2.6 ± 1.1	0.5 ± 0.1	8.3 ± 0.4	54.6 ± 1.7	44.9 ± 3.4	17.4 ± 1.5	31.8 ± 2.9	13.9 ± 1.8	17.4 ± 0.3	912.0 ± 124.6	7.6 ± 0.7
AlCeNPs	2.1 ± 0.6	90.6 ± 1.8	2.5 ± 0.8	5.5 ± 0.9	1.3 ± 1.1	0.3 ± 0.2	7.9 ± 0.5	54.7 ± 2.9	42.5 ± 1.8	16.6 ± 0.8	30.6 ± 2.2	12.7 ± 0.9	17.6 ± 1.0	969.6 ± 86.9	7.9 ± 1.1
6 mg kg^{-1}															
Control	2.3 ± 0.6	90.6 ± 1.9	2.4 ± 0.4	5.2 ± 1.4	0.9 ± 0.6	0.6 ± 0.3	8.1 ± 0.3	53.3 ± 1.5	46.3 ± 4.8	16.5 ± 1.3	30.2 ± 2.9	14.0 ± 0.9	17.6 ± 0.5	1010.6 ± 78.5	7.3 ± 0.3
S-AIONPs	4.7 ± 0.9	89.4 ± 1.7	3.5 ± 0.6	5.2 ± 0.7	1.9 ± 1.9	0.5 ± 0.1	8.4 ± 0.2	52.8 ± 1.6	44.3 ± 1.6	14.5 ± 0.8	27.5 ± 1.0	12.1 ± 0.4	17.8 ± 0.4	1161.7 ± 72.2	7.4 ± 0.8
L-AIONPs	4.4 ± 0.8	90.1 ± 1.4	3.1 ± 0.4	5.5 ± 0.6	1.3 ± 0.8	0.6 ± 0.1	7.9 ± 0.5	52.7 ± 1.5	42.8 ± 1.7	15.6 ± 0.6	31.3 ± 2.4	13.2 ± 1.1	17.9 ± 0.4	934.6 ± 49.9	7.4 ± 0.5
AlCeNPs	2.5 ± 0.9	91.4 ± 1.5	2.7 ± 0.7	4.8 ± 0.5	1.5 ± 0.8	0.4 ± 0.1	7.7 ± 0.6	53.8 ± 1.1	41.6 ± 3.0	16.1 ± 0.6	30.0 ± 0.9	12.5 ± 1.2	17.6 ± 0.3	982.6 ± 82.3	7.7 ± 0.6

AlCeNPs, aluminum cerium oxide nanoparticles; BA, basophils; EO, eosinophils; HCT, hematocrit; Hb, hemoglobin; L-AIONPs, long aluminum oxide nanoparticles; LY, lymphocytes; MCH, mean corpuscular hemoglobin; MCHC, mean corpuscular hemoglobin concentration; MCV, mean corpuscular volume; MO, monocytes; MPV, mean platelet volume; NE, neutrophils; PLT, platelet; RBC, red blood cells; RDW, red blood cell distribution width; S-AIONPs, short aluminum oxide nanoparticles; WBC, white blood cells.

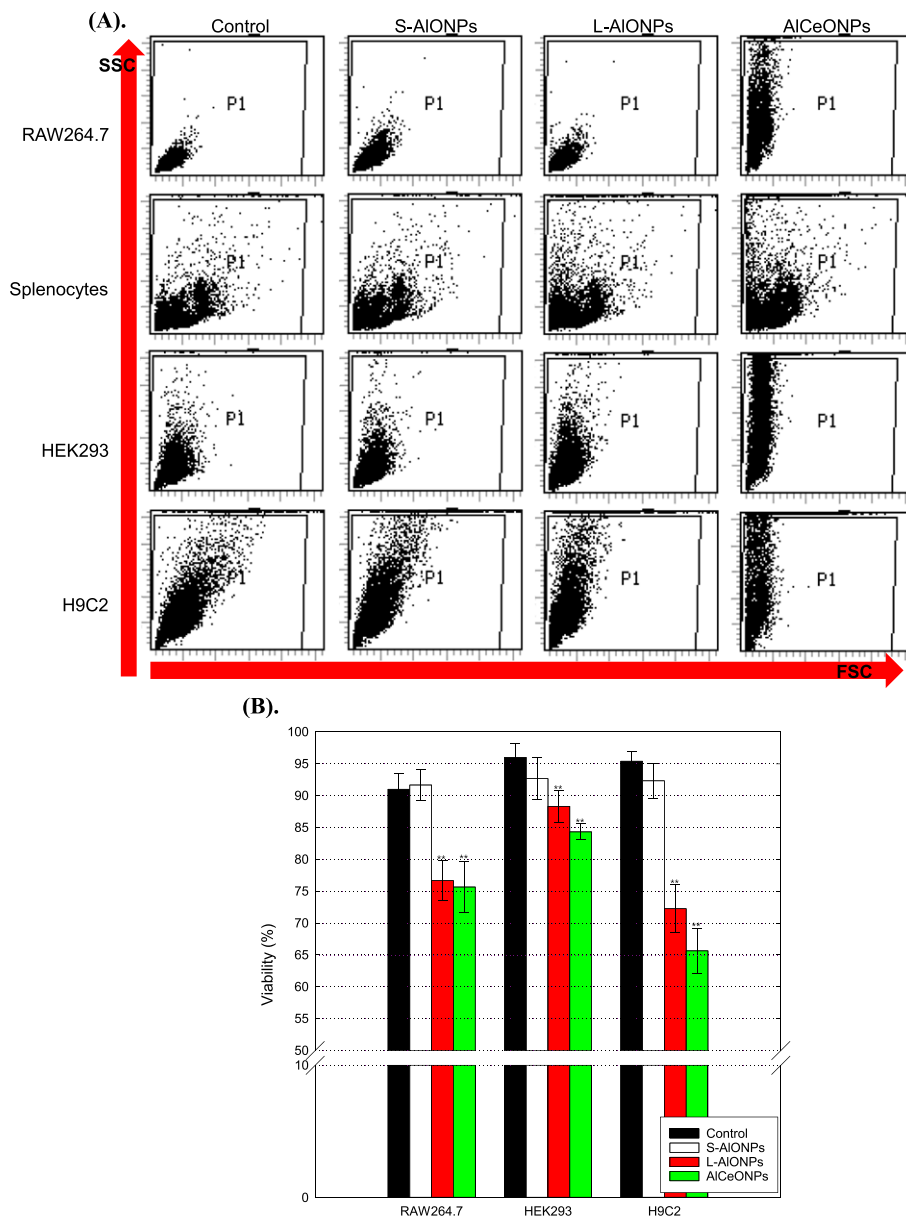


FIGURE 3 Cellular uptake and cytotoxicity. Three types of Al-NPs ($20 \mu\text{g ml}^{-1}$) were treated to four types of cells derived from the target organs, primary splenocytes, H9C2 cells (rat cardiomyocytes), HEK-293 cells (human embryonic kidney cells) and RAW264.7 cells (murine peritoneal macrophage cells), for 24 h, and each experiment was independently performed three times. (A) cellular uptake. Harvested cells were stained with Annexin V and propidium iodide and cellular uptake was expressed with the cell distribution obtained by fluorescence-activated cell sorter analysis. All data showed similar trends, and representative data were presented. (B) cytotoxicity. Viability was measured by trypan blue exclusion staining, and the data indicate the mean \pm SD of three independent experiments. As their size was too small, we failed to obtain stable viability data of splenocytes using an automatic cell counter system. Al-NPs, aluminum nanoparticles; AlCeONPs, aluminum cerium oxide nanoparticles; FSC, forward scatter; L-AIONPs, long aluminum oxide nanoparticles; S-AIONPs, short aluminum oxide nanoparticles; SSC, side scatter

ionization of AIONPs in biological fluids, at least in part. Additionally, in this study, the cellular uptake and cytotoxicity of three types of Al-NPs seemed to be closely associated with their surface area, although we did not identify any direct evidence for the relationship with bioaccumulation following repeated oral administration. Therefore, we propose that surface area of the manufactured NPs can be considered as a key factor in predicting toxicity of NPs, although properties of NPs can be transformed in the biological system.

Collectively, we suggest that the physicochemical properties of NPs should be carefully examined prior to the release into the market to prevent unexpected adverse health effects. Additionally, the surface

area of manufactured NPs can be considered as a key factor in the prediction of the toxicity of NPs, although these properties may be altered in biological systems.

ACKNOWLEDGEMENTS

This work was supported by the Basic Science Research Program, through the National Research Foundation of Korea funded by the Ministry of Education, Science and Technology. (2011-35B-E00011). This study was also supported by the R&D Center for Valuable Recycling (Global-Top R&BD Program) of the Ministry of Environment (project no. R2-17_2016002250005).

CONFLICT OF INTEREST

The authors did not report any conflict of interest.

ORCID

Eun-Jung Park  <http://orcid.org/0000-0002-3723-5351>

REFERENCES

- Alarifi, S., Ali, D., & Alkahtani, S. (2015). Nanoalumina induces apoptosis by impairing antioxidant enzyme systems in human hepatocarcinoma cells. *International Journal of Nanomedicine*, *10*, 3751–3760.
- Alshatwi, A. A., Subbarayan, P. V., Ramesh, E., Al-Hazzani, A. A., Alsaif, M. A., & Alwarthan, A. A. (2013). Aluminium oxide nanoparticles induce mitochondrial-mediated oxidative stress and alter the expression of antioxidant enzymes in human mesenchymal stem cells. *Food Additives & Contaminants. Part A, Chemistry, Analysis, Control, Exposure & Risk Assessment*, *30*, 1–10.
- Arya, A., Gangwar, A., Singh, S. K., Roy, M., Das, M., Sethy, N. K., & Bhargava, K. (2016). Cerium oxide nanoparticles promote neurogenesis and abrogate hypoxia-induced memory impairment through AMPK-PKC-CBP signaling cascade. *International Journal of Nanomedicine*, *11*, 1159–1173.
- Bailey, Z. S., Nilson, E., Bates, J. A., Oyalowo, A., Hockey, K. S., Sajja, V. S. S., ... Rzigalinski, B. A. (2016). Cerium oxide nanoparticles improve outcome after in vitro and in vivo mild traumatic brain injury. *Journal of Neurotrauma*. <https://doi.org/10.1089/neu.2016.4644>. Epub ahead of print
- Bakand, S., Hayes, A., & Dechskulthom, F. (2012). Nanoparticles: A review of particle toxicology following inhalation exposure. *Inhalation Toxicology*, *24*(2), 125–135.
- Cherginets, V. L., Baumer, V. N., Galkin, S. S., Glushkova, L. V., Rebrova, T. P., & Shtitelman, Z. V. (2006). Solubility of Al₂O₃ in some chloride-fluoride melts. *Inorganic Chemistry*, *45*(18), 7367–7371.
- Doshi, R., Braida, W., Christodoulatos, C., Wazne, M., & O'Connor, G. (2008). Nano-aluminum: Transport through sand columns and environmental effects on plants and soil communities. *Environmental Research*, *106*(3), 296–303.
- Duffin, R., Tran, L., Brown, D., Stone, V., & Donaldson, K. (2007). Proinflammogenic effects of low-toxicity and metal nanoparticles in vivo and in vitro: Highlighting the role of particle surface area and surface reactivity. *Inhalation Toxicology*, *19*(10), 849–856.
- Ferreira, P. C., Piai Kde, A., Takayanagui, A. M., & Segura-Muñoz, S. I. (2008). Aluminum as a risk factor for Alzheimer's disease. *Revista Latino-Americana de Enfermagem*, *16*, 151–157.
- Franke, M. D., Ernst, W. R., Myerson, A. S. (1987). Kinetics of dissolution of alumina in acidic solution. *AIChE Journal*, *33*(2), 267–273.
- Fröhlich, E., & Roblegg, E. (2016). Oral uptake of nanoparticles: Human relevance and the role of in vitro systems. *Archives of Toxicology*, *90*(10), 2297–2314.
- Higashisaka, K., Nagano, K., Yoshioka, Y., & Tsutsumi, Y. (2017). Nanosafety research: Examining the associations among the biological effects of nanoparticles and their physicochemical properties and kinetics. *Biological and Pharmaceutical Bulletin*, *40*(3), 243–248.
- Karunakaran, G., Suriyaprabha, R., Rajendran, V., & Kannan, N. (2015). Effect of contact angle, zeta potential and particles size on the in vitro studies of Al₂O₃ and SiO₂ nanoparticles. *IET Nanobiotechnology*, *9*, 27–34.
- Li, X., Liu, W., Sun, L., Aifantis, K. E., Yu, B., Fan, Y., ... Watari, F. (2015). Effects of physicochemical properties of nanomaterials on their toxicity. *Journal of Biomedical Materials Research. Part A*, *103*(7), 2499–2507.
- Li, Y., Yu, S., Wu, Q., Tang, M., Pu, Y., & Wang, D. (2012). Chronic Al₂O₃-nanoparticle exposure causes neurotoxic effects on locomotion behaviors by inducing severe ROS production and disruption of ROS defense mechanisms in nematode *Caenorhabditis elegans*. *Journal of Hazardous Materials*, *219*–220, 221–230.
- Lo, J. H., Kwon, E. J., Zhang, A. Q., Singhal, P., & Bhatia, S. N. (2016). Comparison of modular PEG incorporation strategies for stabilization of peptide-siRNA nanocomplexes. *Bioconjugate Chemistry*, *27*(10), 2323–2331.
- Lu, S., Duffin, R., Poland, C., Daly, P., Murphy, F., Drost, E., ... Donaldson, K. (2009). Efficacy of simple short-term in vitro assays for predicting the potential of metal oxide nanoparticles to cause pulmonary inflammation. *Environmental Health Perspectives*, *117*(2), 241–247.
- Nel, A. E., Mädler, L., Velegol, D., Xia, T., Hoek, E. M., Somasundaran, P., ... Thompson, M. (2009). Understanding biophysicochemical interactions at the nano-bio interface. *Nature Materials*, *8*(7), 543–557.
- Mao, B. H., Tsai, J. C., Chen, C. W., Yan, S. J., & Wang, Y. J. (2016). Mechanisms of silver nanoparticle-induced toxicity and important role of autophagy. *Nanotoxicology*, *10*(8), 1021–1040.
- Marques, M. R. C., Loebenberg, R., & Almukainzi, M. (2011). Simulated biological fluids with possible application in dissolution testing. *Dissolution Technologies*, *8*, 15–28.
- Najafi, R., Hosseini, A., Ghaznavi, H., Mehrzadi, S., & Sharifi, A. M. (2017). Neuroprotective effect of cerium oxide nanoparticles in a rat model of experimental diabetic neuropathy. *Brain Research Bulletin*, *131*, 117–122.
- Pakrashi, S., Dalai, S., Humayun, A., Chakravarty, S., Chandrasekaran, N., & Mukherjee, A. (2013). *Ceriodaphnia dubia* as a potential bio-indicator for assessing acute aluminum oxide nanoparticle toxicity in fresh water environment. *PLoS One*, *8*(9), e74003
- Pakrashi, S., Dalai, S., Prathna, T. C., Trivedi, S., Myneni, R., Raichur, A. M., ... Mukherjee, A. (2013). Cytotoxicity of aluminium oxide nanoparticles towards fresh water algal isolate at low exposure concentrations. *Aquatic Toxicology*, *132*–133, 34–45.
- Park, E. J., Choi, J., Park, Y. K., & Park, K. (2008). Oxidative stress induced by cerium oxide nanoparticles in cultured BEAS-2B cells. *Toxicology*, *245*(1–2), 90–100.
- Park, E. J., Jeong, U., Yoon, C., & Kim, Y. (2017). Comparison of distribution and toxicity of different types of zinc-based nanoparticles. *Environmental Toxicology*, *32*(4), 1363–1374.
- Park, E. J., Kim, H., Kim, Y., & Choi, K. (2011). Repeated-dose toxicity attributed to aluminum nanoparticles following 28-day oral administration, particularly on gene expression in mouse brain. *Toxicological and Environmental Chemistry*, *92*, 120–133.
- Park, E. J., Kim, S. N., Kang, M. S., Lee, B. S., Yoon, C., Jeong, U., ... Kim, J. S. (2016). A higher aspect ratio enhanced bioaccumulation and altered immune responses due to intravenously-injected aluminum oxide nanoparticles. *Journal of Immunotoxicology*, *13*(4), 439–448.
- Park, E. J., Lee, G. H., Shim, J. H., Cho, M. H., Lee, B. S., Kim, Y. B., ... Kim, D. W. (2015). Comparison of the toxicity of aluminum oxide nanorods with different aspect ratio. *Archives of Toxicology*, *89*(10), 1771–1782.
- Park, E. J., Lee, G. H., Yoon, C., Jeong, U., Kim, Y., Cho, M. H., & Kim, D. W. (2016). Biodistribution and toxicity of spherical aluminum oxide nanoparticles. *Journal of Applied Toxicology*, *36*(3), 424–433.
- Park, E. J., Lee, G. H., Yoon, C., & Kim, D. W. (2016). Comparison of distribution and toxicity following repeated oral dosing of different vanadium oxide nanoparticles in mice. *Environmental Research*, *150*, 154–165.
- Park, E. J., Sim, J., Kim, Y., Han, B. S., Yoon, C., Lee, S., ... Kim, J. H. (2015). A 13-week repeated-dose oral toxicity and bioaccumulation of aluminum oxide nanoparticles in mice. *Archives of Toxicology*, *89*(3), 371–379.
- Prabhakar, P. V., Reddy, U. A., Singh, S. P., Balasubramanyam, A., Rahman, M. F., Indu Kumari, S., ... Mahboob, M. (2012). Oxidative stress induced by aluminum oxide nanomaterials after acute oral treatment in Wistar rats. *Journal of Applied Toxicology*, *32*(6), 436–445.
- Radziun, E., Dudkiewicz Wilczyńska, J., Książek, I., Nowak, K., Anuszczyńska, E. L., Kunicki, A., ... Ząbkowski, T. (2011). Assessment of the cytotoxicity of aluminium oxide nanoparticles on selected mammalian cells. *Toxicology In Vitro*, *28*(8), 1694–1700.

- Shah, S. A., Yoon, G. H., Ahmad, A., Ullah, F., Ul Amin, F., & Kim, M. O. (2015). Nanoscale-alumina induces oxidative stress and accelerates amyloid beta (A β) production in ICR female mice. *Nanoscale*, *7*(37), 15225–15237.
- Shrivastava, R., Raza, S., Yadav, A., Kushwaha, P., & Flora, S. J. (2014). Effects of sub-acute exposure to TiO₂, ZnO and Al₂O₃ nanoparticles on oxidative stress and histological changes in mouse liver and brain. *Drug and Chemical Toxicology*, *37*(3), 336–347.
- Solfrizzi, V., Colacicco, A. M., D'Introno, A., Capurso, C., Parigi, A. D., Capurso, S. A., ... Panza, F. (2006). Macronutrients, aluminium from drinking water and foods, and other metals in cognitive decline and dementia. *Journal of Alzheimers Disease*, *10*(2–3), 303–330.
- Srikanth, K., Mahajan, A., Pereira, E., Duarte, A. C., & Venkateswara Rao, J. (2015). Aluminium oxide nanoparticles induced morphological changes, cytotoxicity and oxidative stress in Chinook salmon (CHSE-214) cells. *Journal of Applied Toxicology*, *35*(10), 1133–1140.
- Tripathi, S., Mahdi, A. A., Nawab, A., Chander, R., Hasan, M., Siddiqui, M. S., ... Bajpai, V. K. (2009). Influence of age on aluminum induced lipid peroxidation and neurolipofuscin in frontal cortex of rat brain: A behavioral, biochemical and ultrastructural study. *Brain Research*, *1253*, 107–116.
- Utembe, W., Potgieter, K., Stefaniak, A. B., & Gulumian, M. (2015). Dissolution and biodurability: Important parameters needed for risk assessment of nanomaterials. *Particle and Fibre Toxicology*, *12*, 11.
- Wagner, A. J., Bleckmann, C. A., Murdock, R. C., Schrand, A. M., Schlager, J. J., & Hussain, S. M. (2007). Cellular interaction of different forms of aluminum nanoparticles in rat alveolar macrophages. *Journal of Physical Chemistry B*, *111*(25), 7353–7359.
- Willhite, C. C., Karyakina, N. A., Yokel, R. A., Yenugadhathi, N., Wisniewski, T. M., Arnold, I. M., ... Krewski, D. (2014). Systematic review of potential health risks posed by pharmaceutical, occupational and consumer exposures to metallic and nanoscale aluminum, aluminum oxides, aluminum hydroxide and its soluble salts. *Critical Reviews in Toxicology*, *44*(Suppl. 4), 1–80.
- Zhang, Q., Xu, L., Wang, J., Sabbioni, E., Piao, L., Di Gioacchino, M., & Niu, Q. (2013). Lysosomes involved in the cellular toxicity of nano-alumina: Combined effects of particle size and chemical composition. *Journal of Biological Regulators & Homeostatic Agents*, *27*(2), 365–375.

SUPPORTING INFORMATION

Additional Supporting Information may be found online in the supporting information tab for this article.

How to cite this article: Park E-J, Lee G-H, Yoon C, et al. Tissue distribution following 28 day repeated oral administration of aluminum-based nanoparticles with different properties and the in vitro toxicity. *J Appl Toxicol*. 2017;37:1408–1419. <https://doi.org/10.1002/jat.3509>